

Aspect sensitivity of VHF echoes from field aligned irregularities in meteor trails and thin ionization layers

Q. H. Zhou¹, Y. T. Morton¹, J. D. Mathews², and D. Janches^{2, 3}

¹Electrical and Computer Engineering Department, Miami University, Oxford, OH, USA

²CSSL, Pennsylvania State University, University Park, PA, USA

³Arecibo Observatory, Arecibo, Puerto Rico

Received: 29 September 2003 – Published in Atmos. Chem. Phys. Discuss.: 2 February 2004

Revised: 28 April 2004 – Accepted: 28 April 2004 – Published: 7 May 2004

Abstract. The aspect sensitivity of VHF echoes from field aligned irregularities (FAI) within meteor trails and thin ionization layers is studied using numerical models. Although the maximum power is obtained when a radar is pointed perpendicular to the field line ($\perp \mathbf{B}$), substantial power can be obtained off the $\perp \mathbf{B}$ direction if the ionization trail/layer is thin. When the FAI length along \mathbf{B} is 20 m, the power observed 6° off $\perp \mathbf{B}$ is about 10 db below that perpendicular to the \mathbf{B} direction. Meteoric FAI echoes can potentially be used to determine the diffusion rate in the mesopause region. Based on the aspect sensitivity analysis, we conclude that the range spread trail echoes far off $\perp \mathbf{B}$ observed by powerful VHF radars are likely due to overdense meteors. Our simulation also shows that ionospheric FAI echoes can have an altitude smearing effect of about 4 km if the vertical extension of a FAI-layer is around 100 m, which has often been observed at Arecibo. The altitude smearing effect can account for the fact that the Es-layers observed by the Arecibo incoherent scatter radar are typically much narrower than FAI-layers and the occurrence of double spectral peaks around the Es-layer altitude in FAI echoes.

1 Introduction

Meteor trains had been largely considered to diffuse isotropically (e.g. McKinley, 1961) although the effect of the geomagnetic field (\mathbf{B}) on meteoric diffusion has been studied both experimentally and theoretically (Jones, 1991, and references therein). Jones' (1991) steady-state solution suggests that diffusion is severely inhibited in the direction normal to the plane of \mathbf{B} and the meteor trail. This aspect of anisotropy on diffusion has been further discussed by Robson (2001) and Elford (2004). Recent VHF and UHF ob-

servations demonstrate that field aligned irregularities (FAI), which is a result of plasma instability in the presence of \mathbf{B} field, can occur in meteor trails (Chapin and Kudeki, 1994; Zhou et al., 2001; Close et al., 2002). In particular, the observations by Zhou et al. show that practically every meteor trail contains FAI, including those meteors at altitudes as low as 80 km. Recent theoretical simulations by Oppenheim et al. (2000) and Dyrud et al. (2001) include the instability generated by the polarization electric field and the steep density gradient characteristic of meteor trails. Dyrud et al. (2001) suggest that $\perp \mathbf{B}$ diffusion in the presence of plasma instability can be even faster than along \mathbf{B} in the first few milliseconds after the passage of a meteoroid. It is clear that the existence of plasma instability and FAI presents both challenges and opportunities for aeronomy studies involving meteor trails.

The first intent of this study is to analyze the aspect sensitivity of meteoric FAI and explore the possibility of using FAI echoes to obtain diffusion rate. A useful concept for coherent scattering is the Fresnel length, which is the longest scattering length over which the maximum echo phase change is less than $\pi/2$. In general, if the FAI extension along \mathbf{B} is much larger than the Fresnel length, scattering from off $\perp \mathbf{B}$ directions is much weaker than that from the $\perp \mathbf{B}$ direction. However, if the FAI is confined within a limited space, as in the case of meteor trails, significant echo power can be observed off $\perp \mathbf{B}$ directions. The analysis of aspect sensitivity can yield insight into the diffusion process and potentially lead to the determination of plasma diffusivity rate and temperature in the mesopause region. In Sect. 2, we will describe our numerical model and present simulation results applicable to meteor trails.

FAI exist in the nighttime background ionosphere as well. The second intent of this report is to quantitatively examine aspect sensitivity of ionospheric FAI-layers, and discuss potential observational effects of the off $\perp \mathbf{B}$ echoes. There has been a large body of literature regarding the observations

Correspondence to: Q. H. Zhou
(Zhouq@muohio.edu)

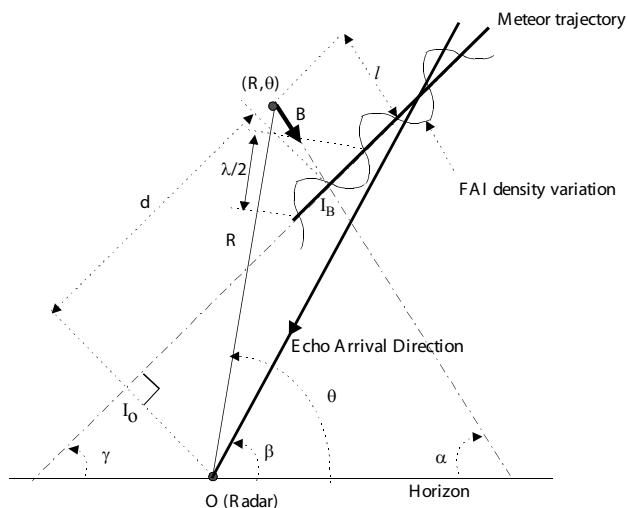


Fig. 1. Radar scattering geometry from a field aligned structure for a meteor trail. The geomagnetic field line, \mathbf{B} , has a dip angle of α . The sinusoidal structure, having a period matching the radar half-wavelength, is the electron density variation caused by plasma instability. The meteor trajectory is assumed to be in the plane containing \mathbf{B} and the radar pointing direction, or the echo arrival direction. The radar pointing direction and the meteor trajectory have an elevation angle of β and γ , respectively. The polar coordinate has the radar location as the origin and the coordinate of an arbitrary point used for integration is (R, θ) . I_B is the intersection of the meteor trajectory and the \mathbf{B} line containing (R, θ) . I_o is the perpendicular intersection of the meteor trajectory and the line passing through O . The distance between (R, θ) and I_B is defined as l and the distance between I_B and I_o is d .

and generations of ionospheric FAI in the nighttime E-region. Recent observations of ionospheric FAI include those of Chu and Wang (1999), Hysell and Burcham (2000), Urbina et al. (2000), Woodman and Chau (2001) and references therein. Middle latitude ionospheric FAI are believed to result from the steep gradient of sporadic E- (Es-) layers and a discussion on various seeding mechanisms can be found in Larsen (2000). Compared with their meteoric counterpart, ionospheric FAI echoes are likely more aspect sensitive because their generally larger horizontal and vertical extension. Nevertheless, ionization layers are often observed to have a vertical thickness less than a few hundred meters by the Arecibo incoherent scatter radar (Mathews et al., 1997). If FAI-layers exist within such thin Es-layers, off $\perp\mathbf{B}$ scatterings can produce visible radar echoes. In the third section of this study, we investigate the echo power variation at different radar look direction for various FAI-layer thicknesses and discuss the potential observational effects of scatterings from non- $\perp\mathbf{B}$ directions.

2 Meteoric FAI echoes aspect sensitivity and their potential applications

2.1 Aspect sensitivity of meteoric FAI echo

A two dimensional meteoric FAI scattering geometry is shown in Fig. 1. To simplify our analysis, we made the following three assumptions: 1) The FAI density can be represented by a sinusoidal variation in the $\perp\mathbf{B}$ direction. The period of the sinusoidal variation is such as to maximize the echo power, which requires that the projection of the spatial period in the echo direction (\mathbf{k}) be half-wavelength. Although the density variation in reality is far more complicated than assumed here, they are nevertheless the superposition of various spatial Fourier components. The spatial components other than those close to the radar half-wavelength do not contribute to the total echo power. A discussion on the range of spatial components that contribute to the scattering power is found in the last section of the paper. 2) The electron density along \mathbf{B} is assumed to decay exponentially from the meteor trajectory point. This assumption is based on the classical ambipolar diffusion equation, assuming that the FAI formation process does not affect the diffusion along \mathbf{B} . 3) Meteor trails lie within the plane containing \mathbf{B} and \mathbf{k} , which is denoted as $\mathbf{k}\hat{\perp}\mathbf{B}$. Although this is not a realistic assumption, the effect of the off $\mathbf{k}\hat{\perp}\mathbf{B}$ meteors is such that a different spatial period along the trajectory actually produces the coherent echoes. This effect should not affect the aspect sensitivity if the FAI extension along \mathbf{B} remains the same for the different spatial periods.

With the geometry in Fig. 1 and the above assumptions, the electron density that gives rise to the coherent scattering at an elevation angle β , which we define as the echo arrival angle, can be described as

$$q = n_o e^{-\left(\frac{2l}{L_B}\right)^2} \left(1 + \cos\left(\frac{4\pi \cos(\beta - \lambda)}{\lambda} d\right) \right), \quad (1)$$

where:

- n_o : the peak electron density at the center of the trail;
- l : the distance variable between an arbitrary point (R, θ) in space and the meteoroid trajectory along \mathbf{B} ;
- L_B : the FAI length along \mathbf{B} ;
- γ : the elevation angle of the meteor trajectory;
- λ : the radar wavelength;
- d : the distance variable along the meteor trajectory measured from the closest point to the radar to the field line of (R, θ) .

Variables l and d are related to the independent variables (R, θ) by

$$l \sin(\alpha + \gamma) = R \sin(\theta - \gamma) - L_o \quad (2)$$

and

$$d = R \cos(\theta - \gamma) + l \cos(\gamma + \alpha), \quad (3)$$

where L_0 is the shortest distance from the radar to the meteor trajectory and α is the dip angle.

The electric field at the radar receiver from a underdense plasma having a two-dimensional electron density distribution $q(R, \theta)$ can be generally written as

$$E \propto \iint \frac{G(\theta)q(R, \theta)e^{j(\omega t - \frac{4\pi}{\lambda} R)}}{R^2} R dR d\theta, \quad (4)$$

where G is the gain of the antenna and ω is the radar angular frequency (e.g. McKinley, 1961). What we are interested in is the amplitude of the electric field, or alternatively the power, which can be expressed as

$$P \propto |E|^2 \propto \left(\iint \frac{G(\theta)}{R} q(R, \theta) \cos\left(\frac{4\pi}{\lambda} R\right) dR d\theta \right)^2 + \left(\iint \frac{G(\theta)}{R} q(R, \theta) \sin\left(\frac{4\pi}{\lambda} R\right) dR d\theta \right)^2. \quad (5)$$

The above integrals are difficult to evaluate analytically except for circumstances involving simple functions of q . We will evaluate it using numerical solutions. In the following, we will focus on how the power varies with the echo arrival angle, β , for various FAI lengths. For simplicity, we will assume that the radar has a uniform gain pattern because the meteor trail dimension is in general small compared to the radar beamwidth.

2.2 Determining diffusion rate from range spread trail echoes

Both ionospheric and meteoric FAI have been extensively observed by the Kyoto University Middle and Upper (MU) atmosphere radar (e.g. Yamamoto et al., 1994; Zhou et al., 2001). For this reason, our simulations assume $\lambda=6.4$ m and $\alpha=51^\circ$, applicable to MU radar. It should also be noted that Arecibo, another important site where a number of meteoric and ionospheric FAI studies have been carried out, has a dip angle of 47° , very similar to that at the MU radar site. Thus the simulation results presented here are largely applicable to Arecibo as well. The integration interval we use for R is 200 m and the interval for θ is 2° with the meteor trail located in the center of integration at 100 km altitude. Figure 2 shows the scattering power as a function of echo arrival angle β with γ being 39° for various FAI lengths. The power is normalized with respect to that at the $\perp \mathbf{B}$ direction. As expected, the echo is less aspect-sensitive when FAI length along \mathbf{B} is shorter. For a FAI length of 20 m, the power observed at 6° off $\perp \mathbf{B}$ is approximately attenuated by 10 db compared to that at the $\perp \mathbf{B}$ direction. We also examined the power variation as a function of β for different γ values. The aspect sensitivity remains more or less the same as that for $\gamma=39^\circ$

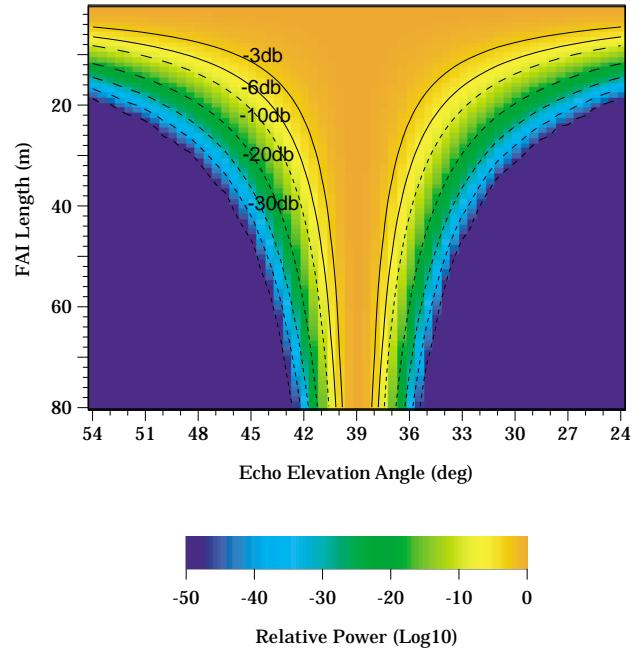


Fig. 2. Normalized echo power as a function of echo arrival angle and FAI length along \mathbf{B} .

if a meteor arrives within $\sim 30^\circ$ from the $\perp \mathbf{B}$ direction. This property makes the study of the FAI diffusive characteristics easier since we can always choose those meteors having a reasonably large line of sight velocity so that γ does not play a major role.

Most of the FAI echo power observed by the MU radar exhibit an exponential decay as a function of time before they disappear. The decay constant in general increases with decreasing altitude. This suggests that the FAI decay process is largely diffusive. The typically large decay constants observed by the MU radar suggest that the ambipolar diffusion $\perp \mathbf{B}$ plays a negligible role before the echoes become invisible to the radar. For instance, if we use an ambipolar diffusion rate of $1 \text{ m}^2/\text{s}$ at 85 km, a 20 db echo is expected to have a lifetime of about 600 ms for specular echoes. The lifetime of a FAI echo is much shorter than 600 ms if isotropic diffusion dominates. Observations show that a 20 dB FAI echo often last several seconds, much longer than 600 ms. It is thus reasonable to assume that diffusion primarily occurs along \mathbf{B} . The instantaneous trail length along \mathbf{B} for a diffusive process can be written as $(L_B/2)^2 = 4Dt + (L_{oB}/2)^2$, where D is the diffusion coefficient, t is the time variable and L_{oB} is the initial trail length along \mathbf{B} . In order to compare the simulation with observation, it is useful to plot the power as a function of L_B^2 , which is directly proportional to t . Figure 3 shows the relative power variation as a function of L_B^2 for various echo arrival angles. The relative power is normalized with respect to the power obtained when all electrons scatter coherently and thus represents the scattering efficiency. One can

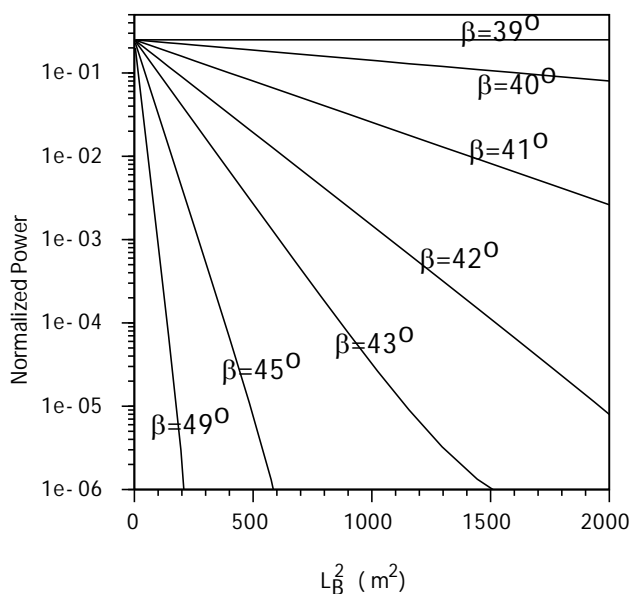


Fig. 3. Normalized echo power as a function of FAI length squared.

easily show that the scattering efficiency saturates at 25% for the sinusoidal density variation assumed. Note that when the radar pointing is $\perp \mathbf{B}$, there is essentially no power decay due to expansion of trail dimension along \mathbf{B} . This is because all the electrons within the Fresnel length $2(R_o\lambda/4)^{1/2} \sim 1000$ m for the $\perp \mathbf{B}$ geometry will scatter coherently, where R_o is the range between the radar and the echoing region and is assumed to be 160 km. Using the interferometry method, such as that described by Yamamoto et al. (1994), one can accurately measure the meteor arrival angle. Designating the e-folding constant measured from the observed power decay as τ_o and the applicable e-folding constant from Fig. 3 as χ , the diffusion rate is $\chi/(16\tau_o)$.

The diffusion constant as determined in the above is a true reflection of the ambipolar diffusion coefficient only if the plasma along each field line remains more or less the same. This assumption is clearly false at the FAI onset period since electrons have to move across the field lines in order to form FAI. In fact, Dyrud et al. (2001) have suggested that the diffusion rate is even larger in the $\perp \mathbf{B}$ direction in the first few milliseconds after ionization has been created. However, for the purpose of diffusivity measurements, the more important period is after the maximum power has been observed, which is typically hundreds of ms after the initial ionization. In any event, in order for the above method to be valid, diffusion along \mathbf{B} has to dominate diffusion $\perp \mathbf{B}$, the FAI dynamics, and chemical loss in controlling the decaying process. Although it is difficult to say theoretically whether diffusion along \mathbf{B} can dominate the other factors, this condition can be rather easily tested observationally. The combined effect of chemical loss, $\perp \mathbf{B}$ diffusion, and the FAI dynamic process can be estimated from echoes that come from the $\perp \mathbf{B}$ direc-

tion since diffusion along \mathbf{B} does not affect the echo power in such a geometry (unless the FAI length is very long). The time constant of the $\perp \mathbf{B}$ echoes at each height have to be much larger than those in the off $\perp \mathbf{B}$ cases in order to derive the diffusion rate. This condition is more likely to be satisfied for echoes relatively far away from the $\perp \mathbf{B}$ direction. The method outlined here, if successful, is more advantageous than using the specular echoes in estimating the diffusion rate since each FAI echo extends many kilometers in altitude while each specular echo is only confined in one range bin. From the diffusion rate, one may further derive the neutral temperature (e.g. Tsutsumi et al., 1994).

As discussed above, observations suggest the $\perp \mathbf{B}$ diffusion rate in RSTE is much smaller than currently accepted ambipolar diffusion rate. If electrodynamic plays a negligible role in the decaying stage of RSTE, observed lifetime of RSTE is indeed consistent with the theoretical prediction that $D_{\perp} < D_{//}$, as suggested by Jones (1991), Robson (2001) and Elford (2004). However, as pointed out by Elford (2004), a more direct and quantitative study of the anisotropy of the diffusion rate is to compare diffusion rates derived from specular echoes observed in both parallel and perpendicular to \mathbf{B} directions. Because of its beam steering capability and the nearly 45° dip angle, MU radar is ideally suited for such a purpose.

2.3 Scattering mechanism of non- $\perp \mathbf{B}$ range spread trail echoes

Although our model simulation applies only to underdense meteors, the general idea applies to overdense meteors as well. The key difference between the underdense FAI and overdense FAI is that in the former the scattering dimension is determined by diffusion while in the latter it is determined by how long the overdense region lasts. The range spread trail echoes (RSTE) observed vertically ($\sim 45^\circ$ off $\perp \mathbf{B}$) by the Arecibo and MU VHF radars (Zhou et al., 1998, 2001) (and perhaps many such echoes presented in McKinley, 1961, as well) are likely associated with overdense echoes for two reasons. First, diffusion would have easily rendered any underdense echoes invisible if the echo arrival angle is as far as 45° off $\perp \mathbf{B}$. Using a diffusion rate of $10 \text{ m}^2/\text{s}$ along \mathbf{B} , applicable for ~ 100 km, an underdense FAI echo will be attenuated by nearly 70 db after 100 ms, making it essentially invisible to the radar. The vertically observed FAI echoes, typically lasting more than 200 ms, clearly did not have such a fast attenuation rate. Second, the longest echo duration in the case of vertically observed RSTE appears to occur near the altitude where the maximum power is detected while that of the $\perp \mathbf{B}$ RSTE occurs near the lowest altitude of the echoing region. Overdense assumption for the vertical RSTE echoes can explain this second feature because the strongest echo region usually has the highest electron density and requires a longer time to diffuse below the overdense threshold. RSTE duration associated with underdense

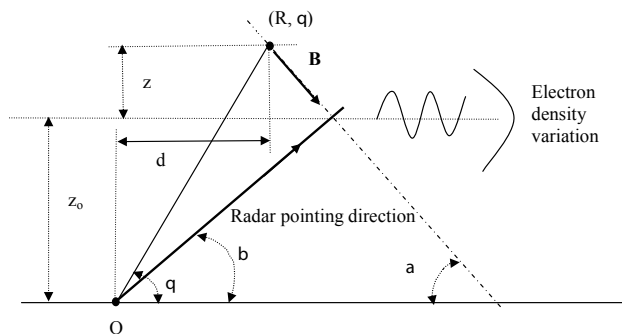


Fig. 4. FAI scattering geometry for a horizontal ionospheric layer. Definitions for α , β and θ are the same as in Fig. 1. Variable d is the horizontal distance from the radar to the integration variable (R, θ) . Variable z is the vertical distance from (R, θ) to the center of the ionospheric layer containing the FAI structure.

plasma tends to be longer at the lower altitudes because of their slower diffusion rate.

The overdense assumption for the far off $\perp \mathbf{B}$ RSTE and the underdense assumption for $\perp \mathbf{B}$ or nearly $\perp \mathbf{B}$ RSTE are also supported by the echo rates observed. Overdense echoes require large meteors. The observed rate of non $\perp \mathbf{B}$ RSTE is typically a few per night for the Arecibo and MU VHF radars while the rate for $\perp \mathbf{B}$ RSTE is over a hundred per hour in the morning hours. In theory, the overdense condition can be due to direct ablation or caused by plasma instability which can change an originally underdense trail into overdense blobs aligned along \mathbf{B} . Nevertheless, the occurrence of plasma instability is essential for the observation of RSTE even in the case where initial meteoric deposition is overdense. In such a case, the initial trail is invisible because the overdense region extends over multiple wavelengths in the radar look direction causing destructive interference. It becomes visible only when the overdense plasma has irregularity or its dimension diminishes to the radar half-wavelength in the radar look direction. This explains the trade-mark time delay between the head-echo and the accompanying RSTE observed by practically all the radars (e.g. McKineley, 1961; Zhou et al., 1998, 2001).

3 Aspect sensitivity of echoes from FAI within horizontal ionization layers

The above analysis can be easily modified to examine the effect of aspect sensitivity of a horizontally extended FAI-layer, which corresponds to $\gamma=0$ in Fig. 1. The new geometry is shown in Fig. 4. For simplicity, we assume that the ionospheric FAI structure extends infinitely in the horizontal. The electron density structure that yields the coherent echo at an elevation angle of β can be written as

$$q \equiv n_o e^{-\left(\frac{2z}{h}\right)^2} \left(1 + \cos\left(\frac{4\pi}{\lambda} d \cos \beta\right)\right) \quad (6)$$

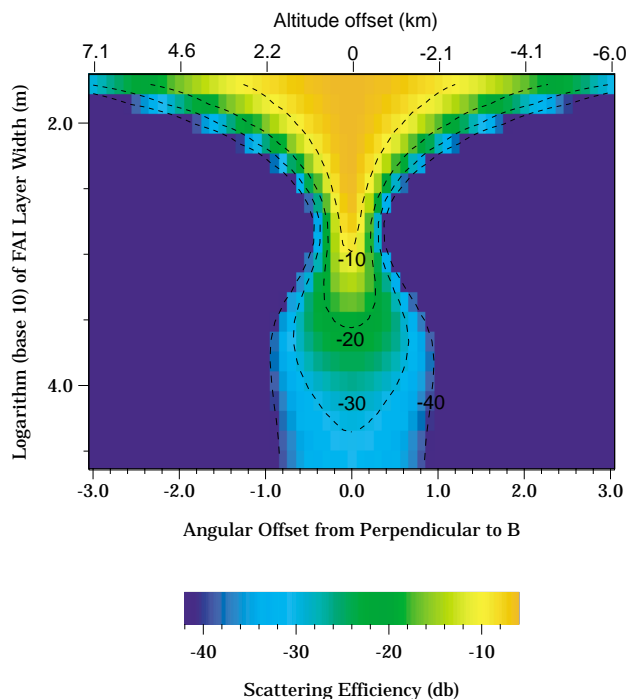


Fig. 5. Normalized echo power as a function of echo arrival angle and vertical FAI-layer width.

for $z < h$, and q is otherwise defined as zero. Here we have changed the variable l along \mathbf{B} for meteoric application to vertical distance variable z , and FAI length L_B to FAI-layer width h since the thickness of FAI-layers in the vertical direction is more commonly used than their length along \mathbf{B} . Definition of other parameters remain the same as those shown in Eq. (1). $z (=l \sin \alpha)$ and d are related to the integration variables R and q by

$$z = R \sin \theta - z_0 \quad (7)$$

and

$$d = R \cos \theta + z \cot \alpha, \quad (8)$$

where Z_o is height of the FAI-layer and is assumed to be 100 km. The equation for radar echo power is the same as Eq. (5). The antenna gain is assumed to decrease exponentially as a function of the distance from the beam center and the 3 db full width is assumed to be 4° .

In Fig. 5, we plot the normalized power as a function of echo arrival angle for various layer widths using the MU radar parameters. The power here is normalized with respect to the power obtained for thin layers at the $\perp \mathbf{B}$ geometry. It is the same as the scattering efficiency plotted in Fig. 3 multiplied by four. The normalized power at the $\perp \mathbf{B}$ geometry remains at unity when the FAI-layer width is less than 800 m for the same reason discussed in the above section. When the FAI width becomes larger than 10 km, the normalized power at the $\perp \mathbf{B}$ direction is reduced to ~ -30 db. The normalized power at the $\perp \mathbf{B}$ geometry for a very wide sinusoidal

structure is about the same as that of a 100 m thin layer at 3° off $\perp\mathbf{B}$ assuming the total number of electrons remain the same. Echoes for very wide FAI-layers do not show strong aspect sensitivity because FAI-region is assumed to extend infinitely in the horizontal direction and part of the FAI-layer is perpendicular to the radar pointing direction.

Echoes coming from the off $\perp\mathbf{B}$ directions cause an altitude smearing effect when they are interpreted to come from the $\perp\mathbf{B}$ direction. The horizontal axis scale on top of Fig. 5 shows the altitude ambiguity, which is the difference between the altitude obtained by assuming the scattering coming from the $\perp\mathbf{B}$ direction and the actual altitude of the FAI-layer. For a FAI-layer width of 100 m, echoes can be observed within 1° off $\perp\mathbf{B}$, corresponding to a 4 km altitude smearing range if we use a 20 db attenuation threshold. Interferometric observations from the MU radar show that it is fairly common to observe echoes 1° off $\perp\mathbf{B}$ (Yamamoto et al., 1994). Although scatterings more than half of a degree off $\perp\mathbf{B}$ have been largely discounted by most authors, Hysell and Burcham (2000) have summarized various potential FAI generating mechanisms and argued that their observations show strong evidence of quasi-point targets moving at a constant altitude. They have modeled the echo intensity as a function of echo arrival angle and found that the 8 db half-width ranges between 0.1° to 0.4° , corresponding to a 20 db half-width of 0.3° to 1.2° . The altitude smearing effect due to off $\perp\mathbf{B}$ scatterings is consistent with the large apparent downward phase velocity often observed by VHF radars. When the scattering regions are localized and spaced in the horizontal direction more or less regularly, background wind would cause apparent periodic radar echoes with large phase velocities. For the MU radar, an 80 m/s southward wind velocity translates to an apparent downward phase velocity of 50 m/s. The predominantly downward phase velocity observed by the MU radar is consistent with the generally southward FAI advection velocities (Yamamoto et al., 1994).

The altitude smearing effect can explain the fact that while many Es-layers observed by the Arecibo incoherent scatter radar are less than 2 km in thickness, FAI echoes are typically much wider. It is generally agreed that FAI originate from the large gradient in the Es-layers. The effective scattering region of a FAI-layer should be largely limited within the Es-layer for two reasons: 1) the Es-layer has a much higher electron concentration than the background ionosphere; and 2) a broad FAI-region has a very low scattering efficiency, as seen from Fig. 5. The simultaneous observations of FAI echoes by a VHF radar and electron density by an incoherent scatter radar reported by Urbina et al. (2000) are particularly useful to explore the relation between FAI and Es echoes. One event presented by Urbina et al. (2000, Fig. 3) shows that the Es-layer is less than 2 km in thickness while the FAI-layer is more than 4 km. The top part of the Es-layer exhibits strong periodic density variation and is about the center altitude of the VHF FAI echo. It is difficult to attribute the echoes observed outside the Es-layer to $\perp\mathbf{B}$ scattering for the

two reasons mentioned above. Instead, we suggest that the effective FAI-region is embedded in only part of the Es-layer. If the strong FAI-region is less than about 100 m, scattering in the off $\perp\mathbf{B}$ directions can account the broad FAI-layer. The 50 m/s southward motion for this event reported by Urbina et al. is also consistent with the ~ 35 m/s apparent layer descending velocity. It should be further pointed out that Es-layers are often patchy. Miller and Smith (1978) showed that the horizontal scale of Es echoes is often less than 300 m at Arecibo. This is consistent with Hysell and Burcham's quasi-point FAI echoes. Further scattering off the geomagnetic meridian plane and the horizontally limited echoing region would potentially make the FAI altitude smearing effect much more severe than discussed here.

The importance of the off $\perp\mathbf{B}$ scattering can be further assessed from the range variations of the Doppler spectra. Because the ionosphere tends to be stratified more in the horizontal than in the vertical direction, the range variation of Doppler shift should be smaller if off $\perp\mathbf{B}$ scattering is significant. In theory, the spectra at any height is a superposition of the $\perp\mathbf{B}$ scattering at the nominal height and off $\perp\mathbf{B}$ scattering from the Es-layer height. The former dominates at heights far away from the Es-layer height (and exactly at the Es height as well) and the latter dominates in the vicinity of the Es-layer height. Presumably, there exist some intermediate heights where the two scattering powers are comparable. Such an effect would be seen as two peaks in the Doppler spectra or as a broadening in the spectral width. The off $\perp\mathbf{B}$ smearing effect may, therefore, explain the double spectral peaks and the spectral broadening found in Fig. 3 of Chu and Wang (1999). Additionally, the altitude smearing effect for low frequency radars is more severe than for high frequency radars. For example, at 24 MHz, we expect the smearing range to double that at 48 MHz for the same FAI-layer width.

4 Discussion and conclusion

In our formulation of FAI, we have ignored the effect of the spatial structures whose wavelengths do not match the radar half-wavelength. Here we briefly consider the contribution from other spatial periods. Let us assume the spatial period to be considered is X , the scattering power, according to Eq. (5), can be written as

$$P_x \propto \left(\iint \frac{G(\theta)}{R} \cos\left(\frac{2\pi}{X}R\right) \cos\left(\frac{4\pi}{\lambda}R\right) dR d\theta \right)^2 + \left(\iint \frac{G(\theta)}{R} \cos\left(\frac{2\pi}{X}R\right) \sin\left(\frac{4\pi}{\lambda}R\right) dR d\theta \right)^2. \quad (9)$$

By defining $\Lambda = \lambda/2X - 1$ and assuming that the dimension of FAI is much larger than the radar wavelength, the above power is found to be

$$P_x \propto \left(\iint \frac{G(\theta)}{R} \cos\left(\frac{4\pi}{X}R\Lambda\right) \cos^2\left(\frac{4\pi}{\lambda}R\right) dR d\theta \right)^2$$

$$+\left(\iint \frac{G(\theta)}{R} \sin\left(\frac{2\pi}{X} R\Lambda\right) \sin^2\left(\frac{4\pi}{\lambda} R\right) dR d\theta\right)^2. \quad (10)$$

If we denote the effective integration range for R as δ_R , P_x is not negligible when compared to $P_{\lambda/2}$ only if $|(4\pi/\lambda)\Lambda\delta_R|$ is of the order of $\pi/2$ or smaller, i.e.

$$\left|\frac{X - \lambda/2}{X}\right| < \frac{\lambda}{8\delta_R}. \quad (11)$$

Since δ_R typically contains many wavelengths, X needs to be confined to a very narrow range around $\lambda/2$ in order to produce significant coherent echoes. We can thus treat the FAI essentially as a half radar wavelength structure for simplicity. It is also of interest to note that since the useful spatial period range is inversely proportional to δ_R linearly, the total coherent signal power remains the same irrespective of the range resolution if the scattering region fills the entire range resolution. We further note that the scattering efficiency discussed in the above section is for that of a sinusoidal structure. The total scattering efficiency of a FAI-layer has to take into account how efficiently the ionosphere is organized into the scattering FAI structure as well.

To summarize, we have analyzed the aspect sensitivity of meteoric and ionospheric FAIs using numerical integrations. If the FAI length is 20 m along the field line, the power observed 6° off $\perp\mathbf{B}$ is 10 db below that in the direction of $\perp\mathbf{B}$. The aspect sensitivity of meteoric FAI is largely not a function of the meteor arrival angle. We argue that $\perp\mathbf{B}$ diffusion is not important in meteoric FAI echoes and the off $\perp\mathbf{B}$ echo decaying characteristics can be potentially used to measure diffusion rate along \mathbf{B} . Such a method, if successful, offers the advantage of being able to measure the diffusion rate over several kilometer altitude range from a single meteor. In addition, we suggest that range spread trail echoes observed far off $\perp\mathbf{B}$ direction are likely due to overdense meteors.

The aspect sensitivity analysis of ionospheric FAI echoes shows that if the FAI echoing region is confined within 100 m vertically, it can have an altitude smearing effect of 4 km for the MU radar parameters. We suggest that the synoptic layer thickness difference between the Es-layers obtained by the Arecibo incoherent scatter radar and FAI-layers can be explained by off $\perp\mathbf{B}$ scattering from narrow FAI structures embedded within the Es-layers. Off $\perp\mathbf{B}$ scattering is also consistent with the large periodic descending phase velocity of FAI echoes associated with Es-layers. In addition, we suggest that off $\perp\mathbf{B}$ scattering can cause spectral broadening or double spectral peak effect. While echo arrival angle may not be as large as 1° off the $\perp\mathbf{B}$ direction, it is potentially very misleading to assume they come exactly from the $\perp\mathbf{B}$ direction. Whether FAI is confined within a very narrow region or extends in a broad range of altitudes needs to be resolved before a true understanding of its generation can be attained.

Acknowledgements. The Arecibo Observatory is the major facility of the National Astronomy and Ionosphere Center, which is operated by Cornell University under a cooperative agreement with the National Science Foundation. The work of Q. H. Zhou and Y. T. Morton was partially supported by NSF grant 0337245.

Edited by: J. Plane

References

- Chapin, E. and Kudeki, E.: Plasma wave excitation on meteor trails in the equatorial electrojet, *Geophys. Res. Lett.*, 21, 2433–2436, 1994.
- Close, S., Oppenheim, M., Hunt, S., and Dyrud, L.: Scattering characteristics of high-resolution meteor head echoes detected at multiple frequencies, *J. Geophys. Res.*, 107, (A10), 1295, doi:10.1029/2002JA009253, 2002.
- Chu, Y.-H. and Wang, C.-Y.: Interferometry investigations of VHF backscatter from plasma irregularity patches in the nighttime E-region using the Chung-Li radar, *J. Geophys. Res.*, 104, 2621–2631, 1999.
- Dyrud, L. P., Oppenheim, M. M., and vom Endt, A. F.: The anomalous diffusion of meteor trails, *Geophys. Res. Lett.*, 28, 2775–2778, 2001.
- Elford, W.: Interactive comment on “Aspect sensitivity of VHF echoes from field aligned irregularities in meteor trails and thin ionization layers” by Zhou, Q. H., Morton, Y. T., Mathews, J. D., and Janches, D.: *Atmos. Chem. Phys. Discuss.*, 4, S192–S195, 2004.
- Jones, W.: Theory of diffusion of meteor trains in the geomagnetic field, *Planet. Space Sci.*, 39, 1283–1288, 1991.
- Larsen, M. F.: A shear instability seeding mechanism for quasiperiod radar echoes, *J. Geophys. Res.*, 105, 24 931–24 940, 2000.
- Mathews, J. D., Sulzer, M. P., and Perillat, P.: Aspects of layer electrodynamics inferred from high-resolution ISR observations of the 80–270 km ionosphere, *Geophys. Res. Lett.*, 24, 1411–1414, 1997.
- McKinley, D. W. R.: *Meteor Science and Engineering*, McGraw-Hill, New York, 1961.
- Miller, K. L. and Smith, L. G.: Incoherent scatter radar observations of irregular structure in mid-latitude sporadic E-layers, *J. Geophys. Res.*, 83, 3761–3775, 1978.
- Oppenheim, M. M., vom Endt, A. F., and Dyrud, L. P.: Electrodynamics of meteor trail evolution in the equatorial E-region ionosphere, *Geophys. Res. Lett.*, 27, 3173–3176, 2000.
- Robson, R. E.: Dispersion of meteor trails in the geomagnetic field, *Phys. Rev. E.*, 63, 026404, 2001.
- Tsutsumi, M., Tsuda, T., and Nakamura, T.: Temperature fluctuations near the mesopause inferred from meteor observations with the middle and upper atmosphere radar, *Radio Sci.*, 29, 599–610, 1994.
- Urbina, J., Kudeki, E., Franke, S. J., González, S., Zhou, Q., and Collins, S. C.: 50 MHz Radar Observations of Mid-Latitude E-Region Irregularities at Camp Santiago, Puerto Rico, *Geophys. Res. Lett.*, 27, 2853–2856, 2000.
- Woodman, R. F. and Chau, J. L.: Equatorial quasiperiodic echoes from field-aligned irregularities observed over Jicamarca, *Geophys. Res. Lett.*, 28, 207–210, 2001.

- Yamamoto, M., Komoda, N., Fukao, S., Tsunoda, R. T., Ogawa, T., and Tsuda, T.: Spatial Structure of the E-Region Field-Aligned Irregularities Revealed by the MU Radar, *Radio Sci.*, 29, 337–348, 1994.
- Zhou, Q., Perillat, P., Cho, J. Y. N., and Mathews, J. D.: Simultaneous meteor echo observations by large aperture VHF and UHF radars, *Radio Sci.*, 33, 1641–1644, 1998.
- Zhou, Q. H., Mathews, J. D., and Nakamura, T.: Implications of meteor observations by the MU radar, *Geophys. Res. Lett.*, 28, 1399–1402, 2001.